

Geodesics in the linearized multipole solution: Distinguishing black holes from naked singularities

J. L. Hernandez-Pastora*

Departamento de Matematica Aplicada and Instituto Universitario de Fisica Fundamental y Matematicas, Universidad de Salamanca, Salamanca, Spain

L. Herrera†

Departamento de Física Teórica e Historia de la Ciencia, Universidad del País Vasco, Bilbao 48940, Spain

J. Ospino‡

Departamento de Matematica Aplicada, Universidad de Salamanca, Salamanca, Spain

(Dated: August 6, 2018)

We analyze the behaviour of geodesic motion of test particles in the spacetime of a specific class of axially symmetric static vacuum solutions to the Einstein equations, hereafter referred to as linearized multipole solution (LM). We discuss about its suitability to describe a quasi-spherical spacetime. The existence of an ISCO (innermost stable circular orbit) very close to the (singular) horizon of the source, is established. The existence of such stable orbit, inner than the one of the Schwarzschild metric, as well as the appearance of a splitting in the admissible region of circular orbits, is shown to be due to the multipole structure of the solution, thereby providing additional potential observational evidence for distinguishing Schwarzschild black holes from naked singularities.

PACS numbers: 04.20.Cv, 04.20.Dw, 97.60.Lf, 04.80.Cc

I. INTRODUCTION

As it follows from the Israel theorem [1], the only static and asymptotically-flat vacuum space-time possessing a regular horizon is the Schwarzschild solution. For all the other Weyl exterior solutions [2–6], the physical components of the Riemann tensor exhibit singularities at the infinite red shift surface. Even though we shall restrict ourselves to the static case, it is worth noting that a result similar to Israel theorem exists for stationary solutions with respect to the Kerr metric [7–9].

Now, sphericity is a common assumption in the description of compact objects, where deviations from spherical symmetry are likely to be incidental rather than basic features of these systems.

Furthermore, if the field produced by a self-gravitating system is not particularly intense (the boundary of the source is much larger than the infinite redshift surface) and fluctuations off spherical symmetry are slight, then there is no problem in representing the corresponding deviations from spherical symmetry (both inside and outside the source) as a suitable perturbation of the spherically symmetric exact solution [10].

However, as the object becomes more and more compact, such perturbative scheme will eventually fail close to the source. Indeed, as is well known [11–16], though

usually overlooked, as the boundary surface of the source approaches the infinite redshift surface, any finite perturbation of the Schwarzschild spacetime, becomes fundamentally different from the corresponding exact solution representing the quasi-spherical spacetime, even if the latter is characterized by parameters whose values are arbitrarily close to those corresponding to Schwarzschild metric. This in turn is just an expression of the Israel theorem.

In other words, for strong gravitational fields, there exists a bifurcation between the perturbed Schwarzschild metric and all the other Weyl metrics (in the case of gravitational perturbations), no matter how small are the multipole moments (higher than monopole) of the source. Examples of such a bifurcation have been brought out in the study of the trajectories of test particles in the γ spacetime [17–24], and in the M-Q spacetime [25, 26], for orbits close to the infinite redshift surface [27],[28].

Due to the bifurcation mentioned above, a fundamental question arises: How should we describe the quasi-spherical space-time resulting from the fluctuations off Schwarzschild?:

- (a) by means of a perturbed Schwarzschild metric producing a black hole
- or
- (b) by means of an exact solution to Einstein equations, whose (radiatable) multipole moments are arbitrarily small, though non-vanishing, and leading to a naked singularity ?

As we shall see here, the quandary above might be

*Electronic address: jlhp@usal.es

†Electronic address: lherrera@usal.es; Also at U.C.V., Caracas

‡Electronic address: j.ospino@usal.es

solved by comparing the behaviour of circular geodesics in either case.

Indeed, in spite of some results obtained in the study of the source of quasi-spherical spacetimes [29], [30], which favor the scenario (b), we are well aware of the fact that, presently, most researchers, favor scenario (a). Nevertheless, the doubt remains, and the very different behaviour of the system implied by the bifurcation mentioned above, opens the way for proposing observational scenarios allowing for distinguishing between black holes and naked singularities. In fact this issue has attracted the attention of many researchers in recent years (see [31–44] and references therein).

However an important open question arises, related to the proposed approach, namely: since there are as many different (physically distinguishable) Weyl solutions as there are different harmonic functions, which among Weyl solutions is the best entitled to describe small deviations from spherical symmetry?

In the past different authors have resorted to different metrics to describe deviations from spherical symmetry; e.g. the γ metric or the M-Q spacetime in [27–30, 43], the Young-Coulter solution [45] in [46], the Quevedo-Mashhoon solution [47] in [48], or the Manko-Novikov solution [49] in [44].

The rationale behind the choice of the γ -metric is based on the fact that it corresponds to a solution of the Laplace equation (in cylindrical coordinates) with a singularity structure similar to that of the Schwarzschild solution (a line segment). In this sense the γ -metric appears as a “natural” generalization of Schwarzschild space-time to the axisymmetric case.

On the other hand, due to its relativistic multipole structure, the M-Q solution (more exactly, a sub-class of this solution M-Q⁽¹⁾ [25]) may be interpreted as a quadrupole correction to the Schwarzschild space-time, and therefore represents a good candidate among known Weyl solutions, to describe small deviations from spherical symmetry.

However it should be obvious that the question above has not a unique answer (there are an infinite number of ways of being non-spherical, so to speak) and therefore in the study of any specific problem, the choice of the corresponding Weyl spacetime has to be reasoned.

In this work we intend to use yet another exact solution of the Weyl family, in order to describe deviations from spherical symmetry. Such a solution is the so called LM metric [50], its properties and the reasons behind its choice to describe a quasi-spherical spacetime are presented in the next section. Next we shall calculate the circular geodesics in that spacetime and compare its behaviour with the spherically symmetric case. The most relevant result emerging from that analysis is the existence of stable innermost circular orbits very close to the (singular) horizon of the source, and inner than the one of the Schwarzschild metric.

II. THE LM SPACETIME

As mentioned in the Introduction we shall carry out a study of circular geodesics in the spacetime of the LM spacetime. Thus, we shall first very briefly revise such a metric and provide arguments justifying its use to describe quasi-spherical (axially symmetric and static) spacetime (see [50] for details). Finally we shall present the multipole structure of the solution.

A. The metric

As is known, the line element of a static and axisymmetric vacuum space-time is represented in Weyl form as follows

$$ds^2 = -e^{2\Psi} dt^2 + e^{-2\Psi} [e^{2\gamma} (d\rho^2 + dz^2) + \rho^2 d\varphi^2] , \quad (1)$$

where Ψ and γ are functions of the cylindrical coordinates ρ and z alone. The metric function Ψ is a solution of the Laplace’s equation ($\Delta\Psi = 0$), and the other metric function γ satisfies a system of differential equations whose integrability condition is just the equation for the function Ψ . Thus, the Weyl family of solutions with a good asymptotical behaviour is given in associated spherical Weyl coordinates $\{r, \theta\}$ as

$$\Psi = \sum_{n=0}^{\infty} \frac{a_n}{r^{n+1}} P_n(\omega) , \quad (2)$$

where $r \equiv \sqrt{\rho^2 + z^2}$, $\omega \equiv \cos \theta = z/r$ and P_n denotes the Legendre polynomial.

Thus the line element now reads

$$ds^2 = -e^{2\Psi} dt^2 + e^{-2\Psi + 2\gamma} (dr^2 + r^2 d\theta^2) + e^{-2\Psi} r^2 \sin^2 \theta d\varphi^2 . \quad (3)$$

Also, as is well known, in spite of the form of (2), coefficients a_n are not the relativistic multipole moments (RMM) of the solution, as defined for static and axisymmetric vacuum solutions by Geroch [51, 52] and Thorne [53]. However the “Newtonian” moments a_n , which provide the so called “Newtonian image” of the solution, can be expressed as functions of the RMM [54–57]. Although the full relations linking both sets of coefficients are extremely complicated, they can be used to obtain relatively simple formulas for the coefficients $\{a_n\}$ in situations where the deviation of the relativistic solution from spherical symmetry is small. This issue has been discussed in some detail in [58], [25], [59].

A solution of the Weyl family that represents the exterior gravitational field of a mass distribution whose multipole structure only possesses mass M and Quadrupole moment Q was found in [25]. This solution (M-Q) has become a useful tool for describing small deviations from the spherically symmetric solution [28, 60–62].

The basic idea underlying the obtention of the M-Q solution is that Q is small since we want to describe slight

deviations from the Schwarzschild solution, and all the RMM of higher order are negligible. This assumption about the RMM higher than Q is supported by the following argument: The Newtonian calculation of the multipole moments of an ellipsoidal mass distribution shows that as we move from lower to higher moments, their magnitudes decrease as powers of the eccentricity of the ellipsoidal configuration (see [58, 63] for details). Then the M-Q solution is constructed as a sum of functions in a power series of the dimensionless quadrupole parameter $q \equiv Q/M^3$ starting at the Schwarzschild solution as the first order, in such a way that the successive powers of q control the desired corrections to the spherical symmetry.

The LM solution [50] was constructed with the same purpose, namely: to describe the gravitational field of a body slightly different from a sphere. However the approach to find it, although similar, is different from the one used for the M-Q solution. In both cases, it should be clear that, describing non-spherical spacetimes, their physical components of the Riemann tensor exhibit singularities at the infinite redshift surface.

The rationale behind the LM solution is the following: When attempting to describe an isolated compact body which is not spherically symmetric, all the RMM appear no matter how small is the deviation from spherical symmetry. Therefore, let us consider that all RMM appear in the solution that we want to construct but let us restrict their magnitudes to be very small, so that we can neglect all terms in the Weyl coefficients whenever a cross prod-

uct of RMM's is involved. This is the origin of the name of the family of solutions: *Linearized Multipole* (LM) solution. It should be observed that due to the linearity of the Laplace equation, the so obtained solution is an exact solution to Einstein equations.

Now, the expression for the metric function of the Weyl family solution endowed with $g + 1$ independent RMM, (the LM-solution), can be written, in prolate spheroidal coordinates [64], as follows

$$\Psi = -\frac{Hx}{x^2 - y^2} - \sum_{n=0}^g Q_{2n}(x)P_{2n}(y) \left[\sum_{j=n}^g H_j C_{2j,2n} \right], \quad (4)$$

where $C_{n,k}$ are the coefficients appearing at the series expansion of any variable as a linear combination of Legendre polynomials in that variable i.e., $\xi^n = \sum_{k=0}^{\infty} C_{n,k} P_k(\xi)$, and

$$H \equiv \sum_{k=0}^g m_{2k} h(k) \quad , \quad H_j \equiv \sum_{k=j}^g m_{2k} h_j(k) \quad , \quad (5)$$

where the parameter $m_{2k} \equiv \frac{M_{2k}}{M^{2k+1}}$ denotes the dimensionless relativistic multipole moment of order 2^{2k} -pole (M_{2k}), whereas the explicit expressions for the coefficients $h_j(k)$ ($\forall k \geq j$, since $h_j(k) = 0$ for $k < j$) and $h(k)$, are:

$$h_j(k) = \frac{1}{2^{4k-1}} (-1)^{k-j-2} \binom{4k+1}{2k} \frac{k^2 + k/2 - j}{(k+1)} \frac{(2k+2j)!}{(2j)!(k+j)!(k-j)!} \quad , \quad h(k) = \frac{1}{2^{2k}(k+1)} \binom{4k+1}{2k} \quad , \quad \forall k > 0 \quad . \quad (6)$$

The parameter H can be calculated in terms of the coefficients H_j as follows:

$$H = \sum_{k=0}^g \frac{m_{2k}}{2^{2k}(k+1)} \binom{4k+1}{2k} = \left[1 - \sum_{j=0}^g \frac{H_j}{2j+1} \right]. \quad (7)$$

In terms of its ‘‘Newtonian image’’, the LM solution can be described by means of an ‘‘object-image’’ whose Newtonian gravitational potential (the gravitational potential corresponding to the Newtonian image, not to confound with the weak field limit of the solution), as well as its Newtonian multipole moments equal the metric function of the solution and the Weyl coefficients respectively. That ‘‘object-image’’ is represented by a kind of ‘‘dumbbell’’ consisting of a bar of length $2M$ with lin-

ear density μ given by an even polynomial of degree $2g$ and two balls at each end of the bar with mass ν (see [50] for details).

The other metric function γ of the line element (1) can be obtained from the metric function Ψ by solving the corresponding field equations

$$\gamma_\rho = \rho(\Psi_\rho^2 - \Psi_z^2) \quad , \quad \gamma_z = 2\rho\Psi_\rho\Psi_z \quad . \quad (8)$$

There already exists an expression for this metric function [64] in terms of the Weyl coefficients of the series Ψ (2), but it is highly complicated to handle and a summation of a series is required to obtain the analytic expression of the metric function. One advantage inherent to the dumbbell description of the solution consists of an integral expression ([65]) for the metric function γ in terms of the density of the dumbbell :

$$\gamma = \int_{-1}^1 dX \int_{-1}^1 dY \frac{\mu^d(X)\mu^d(Y)}{(Y-X)^2} \left[\frac{r^2(1-\omega^2) + (r\omega - XM)(r\omega - YM)}{R(X)R(Y)} - 1 \right], \quad (9)$$

or equivalently,

$$\gamma = -M^2 r^2 (1 - \omega^2) \left[\nu^2 A(r, \omega) + 2\nu(I_- + I_+) + II \right], \quad (10)$$

where the following notation is used $R(X) \equiv \sqrt{r^2 + X^2 M^2 - 2r\omega XM}$, $\mu^d(X)$ represents the density of the dumbbell and

$$\begin{aligned} II &\equiv \int \int_{-1}^1 \frac{\mu(X)\mu(Y) dX dY}{R(X)R(Y) [r^2(1-\omega^2) + (r\omega - XM)(r\omega - YM) + R(X)R(Y)]} \\ I_{\pm} &\equiv \int_{-1}^1 dX \frac{\mu(X)}{r_{\pm} R(X) [r^2(1-\omega^2) + (r\omega - XM)(r\omega \pm M) + r_{\pm} R(X)]} \\ A(r, \omega) &\equiv \frac{1}{4r_-^4} + \frac{1}{4r_+^4} + \frac{1}{r_- r_+ [r^2 - M^2 + r_+ r_-]}. \end{aligned} \quad (11)$$

The fact that the Newtonian image of the LM solution is a dumbbell is quite convenient, since many properties of the solution can be described in terms of the density of the bar. Thus for example, it can be shown that the source of the solution will be prolate (oblate) if μ is smaller (greater) than $1/2$. Also, as we shall see below, the possible existence of an ISCO, inner to the one corresponding to the spherically symmetric case is related to a condition on μ at the origin (32).

B. Multipole structure of the solution

As already mentioned, the RMM of a Weyl solution can be calculated in terms of the coefficients a_n . This relation can be inverted to obtain the Newtonian moments (a_n) in terms of the RMM. The assumption used to construct the LM solution is that every RMM is small, implying that we neglect all the terms with coupling interaction between RMM appearing in the Weyl coefficients a_n (once again it should be emphasized that, due to the linearity of the Laplace equation, the so obtained metric is an exact solution to Einstein equations). With this selection of the coefficients we can consider that the solution possesses a finite number of parameters ($q \equiv m_2, m_{2i}$, with $1 < i \leq g$) that represent each RMM of the solution.

Thus, the first RMM of the solution are the following (odd moments are null because of the equatorial symme-

try):

$$\begin{aligned} M_0 &= M \\ M_2 &= M^3 q \\ M_4 &= M^5 m_4 \\ M_6 &= M^7 \left(m_6 - \frac{60}{77} q^2 \right) \\ M_8 &= M^9 \left(m_8 - \frac{226}{143} q m_4 - \frac{1060}{3003} q^2 - \frac{40}{143} q^3 \right) \\ M_{10} &= M^{11} \left(m_{10} - \frac{28616}{46189} q m_4 - \frac{566}{323} q m_6 - \frac{30870}{46189} m_4^2 \right. \\ &\quad \left. - \frac{19880}{138567} q^2 - \frac{39150}{46189} q^2 m_4 + \frac{146500}{323323} q^3 \right). \end{aligned} \quad (12)$$

III. GEODESICS

We shall now study the geodesic motion of test particles in the spacetime of the LM solution. We shall restrict ourselves to the case of geodesics with constant θ and $\frac{d\varphi}{d\sigma} \neq 0$, i.e., those constrained to a constant hypersurface ($\theta = \theta_0$) with coordinates $\{t, r, \varphi\}$.

Therefore, we obtain on the equatorial plane the following expression (see [61]):

$$\left(\frac{dr}{d\sigma} \right)^2 + V_{eff} = C, \quad (13)$$

where σ denotes the affine parameter along the geodesic, C is a constant and V_{eff} is an effective potential which

can be obtained by integration as follows

$$V_{eff} = \int \frac{k}{g_{11}} \partial_r \ln \left(\frac{g_{11}}{k} \right) dr = -\frac{k}{g_{11}}. \quad (14)$$

with $k \equiv \epsilon - \frac{h^2}{g_{00}} - \frac{l^2}{g_{33}}$, where h and l represent the energy and angular momentum per unit mass respectively, and ϵ denotes the norm of the tangent vector to the geodesic z^α .

From Eqs. (13) and (14) we have that

$$\left(\frac{du}{d\varphi} \right)^2 = \frac{k}{g_{11}} \frac{g_{33}^2}{l^2} u^4, \quad (15)$$

where $u \equiv 1/r$.

The above equations, lead, for the line element (1), to

$$\left(\frac{du}{d\varphi} \right)^2 = \frac{F(r)}{l^2 e^{2\gamma+4\Psi}}, \quad (16)$$

$$V_{eff} = -\frac{F(r)}{e^{2\gamma}}, \quad (17)$$

where the function $F(r) \equiv k e^{2\Psi}$ for timelike geodesics on the equatorial plane is

$$F(r) = -e^{2\Psi} + h^2 - \frac{l^2}{r^2} e^{4\Psi}. \quad (18)$$

When looking for circular orbits we search for the stationary solutions of the autonomous partial differential equation (16), i.e., $\frac{du}{dr} = 0 \iff u = cte$. Hence we can say that the circular orbits are defined by radial values $r = R_i$ where the following condition is satisfied:

$$F(R_i) = \frac{dF}{dr}(R_i) = 0, \quad (19)$$

since the extremals of the effective potential satisfy (prime denotes derivative with respect to r)

$$\begin{aligned} \frac{dV_{eff}}{dr}(R_i) = 0 &= (-F'(R_i) + F(R_i)2\gamma'(R_i)) e^{-2\gamma(R_i)} \\ &\Rightarrow F' \equiv \frac{dF}{dr}(R_i) = 0. \end{aligned} \quad (20)$$

Therefore, the circular orbits can be calculated by means of the function $F(r)$ without using the second metric function γ since the complete effective potential is not needed.

The timelike geodesics described by a pointlike particle around a circular orbit is defined by the zeros of both the function $F(r)$ and its derivative. The orbit $r = R_i$ is stable ($\frac{d^2 V_{eff}}{dr^2} > 0$) if $-F''(R_i) > 0$ (the minimum) and it is unstable ($\frac{d^2 V_{eff}}{dr^2} < 0$) if $-F''(R_i) < 0$ (the maximum). In the above it has been used that

$$\frac{d^2 V_{eff}}{dr^2} = e^{-2\gamma} (-F'' + F'4\gamma' + F2\gamma'' - (2\gamma')^2 F) \quad (21)$$

and hence

$$\frac{d^2 V_{eff}}{dr^2}(R_i) = -e^{-2\gamma(R_i)} F''(R_i). \quad (22)$$

Observe that the specific energy of the geodesic orbit is $E = -z_0$, therefore, since $z_0 = h = \frac{dt}{d\sigma} g_{00} < 0$, the parameter h (with $V_{eff} = 0$ or equivalently $F(R_i) = 0$) denotes, up to a sign, the energy per unit of mass of the test particle and it is fixed once the extremals (R_i) of $F(r)$ are determined:

$$h^2 = e^{2\Psi(R_i)} \left[1 + \frac{l^2}{R_i^2} e^{2\Psi(R_i)} \right]. \quad (23)$$

Also, observe that the conditions for circular orbits (19), (20) determine the values of h and l as follows:

$$l_i^2 = \frac{r^3 \Psi'}{e^{2\Psi}(1-2r\Psi')} \Big|_{r=R_i}, \quad h_i^2 = e^{2\Psi} \frac{1-r\Psi'}{1-2r\Psi'} \Big|_{r=R_i} \quad (24)$$

Then, these parameters are constants of motion for each value of the radial coordinate $r = R_i$. In what follows we shall consider the angular parameter as a function of the radial coordinate r for different circular orbits and hence we introduce the notation

$$L = L(r) \equiv \frac{l^2}{4M^2} = \frac{r^3 \Psi'}{4M^2 e^{2\Psi}(1-2r\Psi')}. \quad (25)$$

A. The spherically symmetric solution

For the forthcoming discussion, it would be convenient to recover the Schwarzschild case, which is well known.

Depending on the value of L the function $-F(r)$ acquires a maximum and a minimum starting from the particular value $L = 3$ for which both extremals coincide at $r_s = 6M$. For large values of L the minimum goes away asymptotically along $r_s/M = 3$. In what follows the notation $\lambda \equiv r_s/M$ shall be used, where r_s denotes the radial Schwarzschild coordinate and it is related to the radial Weyl coordinate r (on the equatorial plane) as follows:

$$s \equiv \frac{r}{M} = \frac{r_s}{M} \sqrt{1 - 2\frac{M}{r_s}}. \quad (26)$$

In figure 1a we plot the parameter L as function of the dimensionless Schwarzschild radial coordinate r_s/M , where the fact that for the circular orbits of the Schwarzschild space-time: $r_s/M = 2L(1 \pm \sqrt{1-3/L})$, has been used. The value of the parameter h is taken to be zero, since it only generates a displacement of the graphic along the vertical axis. There exist certain value h for each extremal R_i , where $F(R_i) = 0$. In figure 1b, $-F(r)$ with its extremals are shown for different values of L .

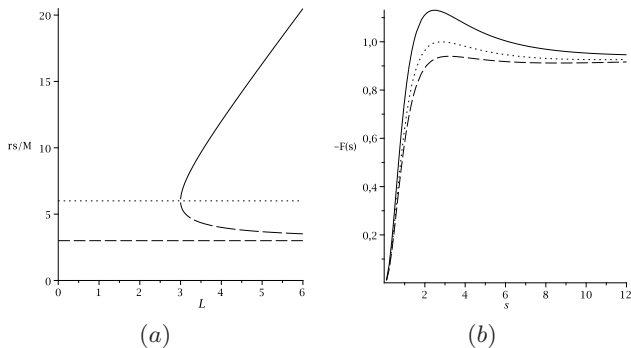


FIG. 1: (a) The plot of the parameter L in terms of the dimensionless Schwarzschild radial coordinate r_s/M . For each value of the parameter L (horizontal axis) the solid line and the long-dashed line provide the points where the function $-F(s)$ acquires the minimum or the maximum respectively. These values define the corresponding radii of the circular stable or unstable orbits respectively. As is known, no matter how large the parameter L would be, the inner unstable orbit is located at $r_s = 3M$ (dashed horizontal line), and the bifurcation point between stable and unstable orbits (the marginally stable orbit) is located at $r_s = 6M$ where the inner stable orbit is reached (shown with a dot line in the graphic). (b) In this graphic the function $-F(s)$ is represented for different values of L . Starting from the solid line and downward, the values of the parameter L are: $L = 5, 4, 3.5$. Let us note that the value $L = 3$ corresponds to the marginally stable orbit, where $F(s)$ has no extremals points but an inflection point.

B. The LM solution

Let us now analyze the situation in the LM solution. To derive the consequences implied by the extremal condition $F'(r) = 0$, we need to solve numerically the following transcendent equation

$$e^{2\Psi} = \frac{r^3}{l^2} \frac{\Psi'}{1 - 2r\Psi'}. \quad (27)$$

Nevertheless, a relevant information can be extracted from the analytical study of the function $-F(r)$ (18). The calculation of that function for the LM solution yields

$$-F(s) = G^{C(s)} e^{A(s)} + \frac{4L}{(\sqrt{s^2+1}+1)^2} G^{2C(s)-1} e^{2A(s)} - h^2 \quad (28)$$

with the notation (for the case $g = 2$)

$$A(s) \equiv -\sqrt{s^2+1}B(s) - \frac{2H}{\sqrt{s^2+1}} \quad (29)$$

$$G \equiv \frac{\sqrt{s^2+1}-1}{\sqrt{s^2+1}+1}, \quad C(s) \equiv H_0 - \frac{1}{2}H_1s^2 + \frac{3}{8}H_2s^4 \quad (30)$$

$$B(s) \equiv H_1 + H_2 \left(\frac{1}{2} - \frac{3}{4}s^2 \right). \quad (31)$$

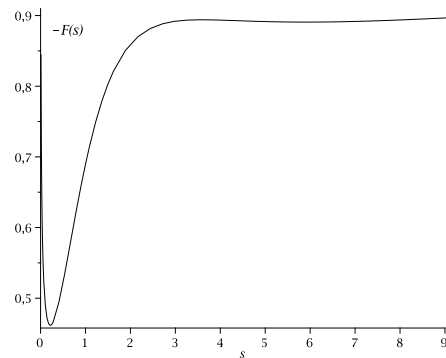
These expressions are easily obtained from the metric function Ψ (4) by considering it on the equatorial plane

($y = 0$) and taking into account that $x = \lambda - 1 = \sqrt{1+s^2}$ (the explicit expression of Ψ in Weyl coordinates can be seen in [50]). Let us note that $e^{2\Psi} = G^{C(s)}e^{A(s)}$ and $G^{2C(s)} = \frac{G^{2C(s)-1}s^2}{(\sqrt{s^2+1}-1)^2}$.

As can be seen in figure 2, the behaviour of the function $-F(r)$ is different from that corresponding to the spherically symmetric case.

Indeed, as shown in that figure, for certain values of the multipole parameters $q \equiv m_2$ and m_4 , the curve clearly shows a minimum close to the origin. This implies the existence of an ISCO, inner to the one corresponding to the spherically symmetric case, and therefore related to the presence of the multipole moments (m_2 and m_4). Let us remember that $r = 0$ corresponds to the infinite redshift surface (26).

FIG. 2: The function $-F(s)$ is represented for the LM solution possessing Monopole, quadrupole and 2^4 -pole moment ($h = 0$ is considered).



If we calculate the behaviour of the function $-F(s)$ when approaching the horizon, we see that this function goes to infinity for certain values of the multipole parameters, thereby exhibiting the existence of a minimum which is absent in the Schwarzschild solution:

$$\lim_{s \rightarrow 0} (-F(s)) = \begin{cases} 0 & , \quad 2H_0 - 1 > 0 \\ \infty & , \quad 2H_0 - 1 < 0 \end{cases}, \quad (32)$$

since $\lim_{s \rightarrow 0} e^{2\Psi} = \lim_{s \rightarrow 0} G^{C(s)}e^A = 0$ because $C(0) = H_0 \equiv 2\mu^{LM}(0) > 0$ (the density of the dumbbell bar is positive definite).

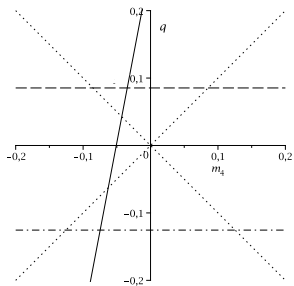
For the case of M-Q⁽¹⁾ solution, i.e. the LM solution with monopole and quadrupole moments alone, the existence of the ISCO is determined by the following range of values of the quadrupole parameter: $q \in [\frac{4}{15}, \frac{8}{15}]$.

For the case of LM solution with monopole, quadrupole and 2^4 -pole moments, the existence of the ISCO is determined by the following range of values of the quadrupole parameter:

$$q \in \begin{cases} [-\frac{32}{255}, -\frac{16}{255}], & m_4 = q \\ [\frac{16}{375}, \frac{32}{375}], & m_4 = -q \end{cases},$$

where we have assumed that the absolute value of both multipole moments are identical (see ([50]) for details). The determination of these ranges of values is obtained from imposing two conditions: the positive definite density condition and $2H_0 - 1 < 0$, that leads to $0 < H_0 < 1/2$ (see the figure 3 for details and a graphical characterization of these ranges).

FIG. 3: The domain of the existence of ISCO in the LM solution is shown. Dotted lines draw the condition assumed on the parameters q and m_4 which are supposed to be of equal magnitude (in absolute value). The continuous line represents the limit (32) $1 - \frac{15}{4}q + \frac{315}{16}m_4 < 0$ for the existence of ISCO, hence the values of q must be situated on top of this line. The intersections of these lines determine the upper value of q if it is negative or the lower bound if it is positive, whereas the other extremes of the ranges are determined by the definite-positive condition of the density (horizontal dashed line and dot-dashed line).



In addition, a more relevant feature of these solutions is obtained from the study of the marginally stable orbit (mso). Indeed, as is known, for a circular (mso) orbit, the angular parameter (as well as the energy) have extremal values. This condition is just equal to $F'' = 0$ as can be seen by taking the derivative of equation (25)

$$\frac{dL}{dr} = 0 \iff 0 = r\Psi'' + 3\Psi' + 4r^2(\Psi')^3 - 6r(\Psi')^2. \quad (33)$$

Therefore, the circular equatorial motion is known to be stable when $L' > 0$ and unstable for $L' < 0$. Let us notice that the epicyclic frequency is proportional to L' , and hence the mso ($L' = 0$) determines the orbit with non horizontal oscillations. The existence of an ISCO, as we have previously shown, can be confirmed when studying the behaviour of L in terms of the orbital radius.

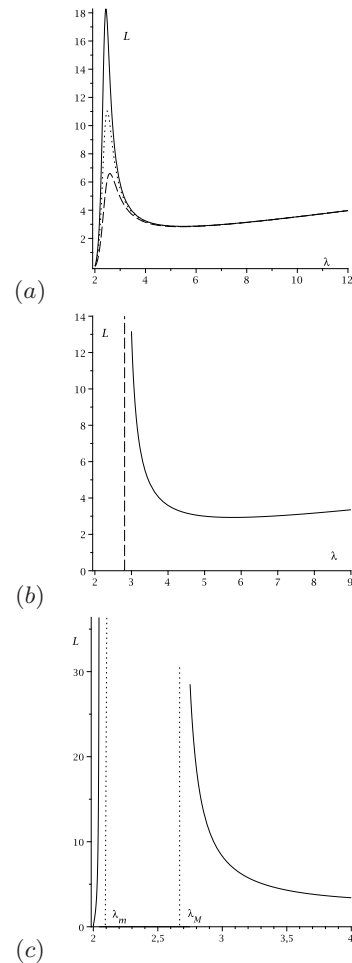
Such a behaviour is displayed in figure 4 using the equation in (25), for different values of the quadrupolar parameter q , for the case of the M- $Q^{(1)}$ solution. For the discussion below an important role will be played by the function $g(r) \equiv 1 - 2r\Psi'$, which is related to L by

$$\frac{dL}{dr} = \frac{1}{4M} \frac{r^3\Psi'' + 3r^2\Psi' + 4r^4(\Psi')^3 - 6r^3(\Psi')^2}{e^{2\Psi}g(r)^2}. \quad (34)$$

The plot of g as function of λ is given in figure 5 for the M- $Q^{(1)}$ and the LM solutions.

The following conclusions emerge from figures 4 and 5:

FIG. 4: Localization of circular orbital radii in terms of the parameter L (in the vertical axis) for different values of the quadrupolar parameter for the M- $Q^{(1)}$ solution. (a) For $q \in (q_c, 8/15]$. Starting from the solid line and downwards the values of the corresponding quadrupolar parameter are $q = 0.4, 0.42, 0.46$. (b) For $q \in (0, 4/15]$. This curve corresponds to $q = 0.2$ where the asymptota is located at $\lambda = 2.8125$ (a smaller value than the corresponding for the Schwarzschild case $\lambda = 3$). (c) For $q \in (4/15, q_c]$. This piece wise curve corresponds to $q = 0.3$ where the asymptotic lines bounding the forbidden region are located at $\lambda_m = 2.0473$ and $\lambda_M = 2.6646$.



- First, we see that stable orbits are located to the left of the maximum, and the right of the minimum (figure 4 (a)) where $L' > 0$. The slope of the curve where $L' < 0$ determines the range of the orbital radius for unstable orbits. The mso is located at the maximum or minimum of the curve (L_+ and L_- respectively). The values of the orbital radius (mso_+ and mso_- for the maximum and minimum respectively) at these two extremals of L correspond to the inflection points of the potential $-F$ for which this function does not possess extremal points. For other values of $L \in (L_+, L_-)$ (at each value of q) the

potential $-F$ will possess one maximum and two minima corresponding to the intersection points of the curves in Figure 4(a) with the horizontal lines $L = cte$.

- Second, figure 4(b) represents the curve for a value of the quadrupolar parameter q where the inner unstable orbit is limited by the asymptotic dashed line, and the inner stable orbit is located at the minimum of the curve. This plot recovers the behaviour of the spherical case but slightly modifying the position of the circular orbits when a quadrupole moment is present. The relevant difference with respect to the spherical case is that a maximum of L (L_+) arises at the value of the radial coordinate mso_- whenever some multipole of the solution, higher than the monopole, is not zero (within a determined range of that multipole parameter), and this fact leads to the existence of stable circular orbits at a radius smaller than those where the other known minima and the maximum appear. In addition, these new stable circular orbits possess smaller values of L and energy h than the former ones.

- Finally, we notice the existence of a splitting (see the figure 4(c)) in the admissible region of circular orbits radius for some values of the multipole moments of our space-time. This fact was already discussed in [44], where by means of numerical methods the authors obtain results that suggest the existence of disconnected non-plunging regions at small radii. The existence of such regions could be tested, for instance, in the presence of accretion disks forming a ring structure around the source. The analytical determination of that region consists of calculating the zeros of the function $g(r)$.

Thus, for some values of q the maximum of L disappears and a region of forbidden circular orbits arises as is shown in figure 4 (c). That region corresponds to the range of values of the radial coordinate leading to $g(r) < 0$ (let us remember that $L \geq 0$, $h^2 \geq 0$). The zeros of the function $g(r)$ (see figure 5) provide the asymptotical behaviour of L at the values λ_m and λ_M (figure 4(c)).

To complement the discussion above it is instructive to take a look at tables I and II, which display the values of different parameters characterizing ISCO's for the LM solution with $g = 1$ (M-Q⁽¹⁾). As mentioned before, if $q \in (0, \frac{4}{15}]$ the behaviour of circular orbits is similar to the spherically symmetric case: the minimum of L (graphic (b) in figure (4) defines the change from stable to unstable orbits, and thereby the minimal value of the radius of the stable circular orbit (mso_-).

The maximum of the orbital radius for the unstable orbit exhibits (as in the Schwarzschild case) an asymptote in the value of λ which is smaller than the corresponding to the spherically symmetric case ($\lambda = 3$).

There exists a critical value for q (q_c) beyond which a gap in the range of possible values of the radius of the circular orbit appears, for which there are not ISCO's. This is clearly indicated in the graphic (c) of figure 4, where the gap is determined by the interval (λ_m, λ_M) for $q \in (\frac{4}{15}, q_c]$.

In the interval $(0, \lambda_m)$ there are ISCO's close to the infinite redshift surface.

For the M-Q⁽¹⁾ solution q_c is given by:

$$q_c = 0.373434, r_s/M = 2.367, \quad (35)$$

that corresponds to the value of q for which $g(r)$ has a single zero (see figure 5).

If $q \in (q_c, \frac{8}{15}]$ there are ISCO's in the interval $(0, L_+)$, with values of the orbital radius smaller than those corresponding to stable circular orbits for L_- where L has a minimum (mso_-).

Three comments are in order at this point:

- It should be stressed that the range of admissible values of the angular momentum $(0, L_+)$ is quite large. Therefore, ISCO's correspond to test particles with a wide range of angular velocities.
- The energies corresponding to ISCO's are smaller than those corresponding to larger values of the orbital radii.
- It should be observed that for the M-Q⁽¹⁾ solution there are ISCO's (inner to $3M$) only for positive values of q (i.e. prolate sources). This important difference between both cases (prolate and oblate) has been brought out before for the γ [27] and the M-Q⁽¹⁾ [28, 62], spacetimes. We ignore what could be (if any) the fundamental physical reason for such a difference.

Finally, table III displays some values of relevant parameters (mso_- , L_- and λ), as well as the interval of non existence of stable circular orbits (λ_m, λ_M) , for the LM solution with quadrupole and 2^4 -pole.

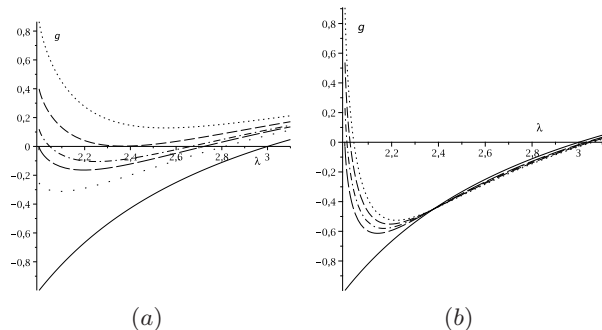
It should be observed that now, unlike the case of the M-Q⁽¹⁾ solution, the function $L(\lambda)$ has no maximal value, implying there exists no mso_+ . Thus, the existence of ISCO's is restricted to the interval $r_s/M \in (0, \lambda_m)$ whenever the quadrupole and the 2^4 -pole are localized within the range mentioned before (33).

Also, the value of λ_m is significantly reduced with respect to the M-Q⁽¹⁾ case, and therefore ISCO's are now very close to the infinite redshift surface ($r_s/M = 2$). At the same time, the range (λ_m, λ_M) increases with respect to the previous case. For values of r_s/M starting from mso_- (minimum of L) we obtain the values of the farthest possible stable circular orbits.

IV. CONCLUSIONS

We have presented a systematic study on the structure of circular geodesics in the LM spacetime. The case has

FIG. 5: Plot of g as function of λ for the $M-Q^{(1)}$ (a) and LM (b) solutions for different values of the multipole parameters. The solid line in both plots corresponds to the Schwarzschild case $q = 0$, whereas the other values of q are: (a) upper dotted line $q = 0.5$, dashed line $q = 0.374 \sim q_c$ and from that line and downwards $q = 0.3, 4/15, 0.2$, The special value $q = 4/15$ corresponds to the lower bound for the existence of ISCO near the horizon. (b) from the solid line $q = m_4 = 0$ and upwards, $q = m_4 = -0.063, -0.08, -0.1, -0.124$.



been made for the use of such spacetime when describing slight deviations from spherical symmetry.

The analysis presented clearly exhibits the difference between the motion in the Schwarzschild and in the LM, spacetimes. In the former case we have a black hole whereas in the latter a naked singularity appears. Our results, as well as those in the references already mentioned, point to a potentially observable evidence allowing to distinguish between the two above mentioned situations. We may summarize such results as follows:

- The presence of multipole moments (higher than the monopole) leads to the presence of ISCO's, closer to the infinite redshift surface than the ones existing in the exactly spherically symmetric case.
- Such multipole moments also produce an interval in the values of radial coordinate within which no stable circular orbits exist.
- Specific numerical values have been presented to illustrate the two abovementioned effects.
- Particularly relevant might be the application of the presented results to studying the dynamics of accretion discs around compact objects, which as it is well known, are assumed to be an essential ingredient of active sources such as X-ray binaries or galactic nuclei (see [66] and references therein). However such a study is out of the scope of this paper.

V. ACKNOWLEDGMENTS

This work was partially supported by the Spanish Ministerio de Ciencia e Innovación under Research Project No. FIS 2012-30926, and the Consejería de Educación of the Junta de Castilla y León under the Research Project Grupo de Excelencia GR234.

TABLE I: Numerical values of characteristic parameters corresponding to ISCO's in the $M-Q^{(1)}$ solution.

q	L	h^2	ISCO(r_s/M)
0	3	0.889	6
0.28	0.1	0.016	2.000
0.28	1.1	0.147	2.001
0.28	2.1	0.269	2.004
0.28	3.1	0.388	2.006
0.28	4.1	0.508	2.007
0.28	5.1	0.626	2.008
0.34	0.1	0.053	2.003
0.34	1.1	0.259	2.041
0.34	2.1	0.433	2.062
0.34	3.1	0.602	2.076
0.34	4.1	0.769	2.086
0.34	5.1	0.935	2.093
0.40	0.1	0.093	2.015
0.40	1.1	0.335	2.104
0.40	2.1	0.535	2.148
0.40	3.1	0.728	2.179
0.40	4.1	0.918	2.202
0.40	5.1	1.106	2.222
0.46	0.1	0.130	2.038
0.46	1.1	0.392	2.174
0.46	2.1	0.606	2.245
0.46	3.1	0.811	2.301
0.46	4.1	1.010	2.352
0.46	5.1	1.202	2.407
0.52	0.1	0.163	2.068
0.52	1.1	0.436	2.248
0.52	2.1	0.657	2.350
0.52	3.1	0.865	2.446
0.52	4.1	1.064	2.577

TABLE II: Extremal values of the marginally stable orbits mso_+ and mso_- with the corresponding value of the angular momentum parameter L for which ISCO's exist, and the range of non existence of stable orbits, for different values of the quadrupole moment, for the M-Q⁽¹⁾ solution.

q	mso_+	L_+	mso_-	L_-	(λ_m, λ_M)	λ
0	-	-	6	3	-	3
0.04	-	-	5.957	2.987	-	2.968
0.08	-	-	5.913	2.973	-	2.934
0.12	-	-	5.868	2.960	-	2.898
0.16	-	-	5.821	2.946	-	2.857
0.20	-	-	5.772	2.931	-	2.812
0.24	-	-	5.722	2.917	-	2.761
0.26	-	-	5.696	2.909	-	2.732
0.28	-	-	5.670	2.902	2.014, 2.701	-
0.30	-	-	5.643	2.894	2.047, 2.665	-
0.32	-	-	5.615	2.886	2.092, 2.623	-
0.34	-	-	5.587	2.878	2.149, 2.571	-
0.36	-	-	5.559	2.870	2.230, 2.498	-
0.37	-	-	5.544	2.866	2.298, 2.434	-
0.374	2.374	7.04e ⁹	5.538	2.865	-	-
0.40	2.435	18.277	5.500	2.854	-	-
0.44	2.540	8.152	5.436	2.837	-	-
0.48	2.645	5.634	5.370	2.820	-	-
0.52	2.753	4.498	5.298	2.801	-	-
8/15	2.789	4.248	5.273	2.795	-	-

TABLE III: The case of LM solution with $g = 2$, i.e, quadrupole and 2⁴-pole moments. Numerical values of the multipole parameters q and m_4 for which ISCO's exist. The value of the marginally stable orbit mso is given with the corresponding value of the angular momentum parameter L .

q	m_4	mso_-	L_-	(λ_m, λ_M)
-0.063	-0.063	6.000	3.0195	2.000, 3.030
-0.08	-0.08	6.000	3.0248	2.0091, 3.038
-0.10	-0.10	6.000	3.0311	2.0224, 3.047
-0.124	-0.124	6.000	3.0386	2.0385, 3.058
0.0427	-0.0427	5.9501	2.9852	2.000, 2.953
0.05	-0.05	5.9414	2.9826	2.0081, 2.943
0.06	-0.06	5.9294	2.9791	2.024, 2.931
0.07	-0.07	5.9173	2.9756	2.044, 2.917
0.085	-0.085	5.8989	2.9702	2.075, 2.899

- [1] W. Israel, *Phys. Rev.* **164**, 1776 (1967).
[2] H. Weyl, *Ann. Physik* **54**, 117 (1918).
[3] H. Weyl, *Ann. Physik* **364**, 185 (1919).
[4] T. Levi-Civita, *Atti. Accad. Naz. Lincei Rend. Classe Sci.Fis. Mat.Nat.* **28**, 101 (1919).
[5] J. L. Synge, *Relativity, The general theory* (North-Holland Publ. Co, Amsterdam) (1960).
[6] Stephani H. *et al*, *Exact Solutions to Einstein's Field Equations*. Cambridge University Press. 2nd Edition, (2003)
[7] B. Carter, *Phys. Rev. Lett.* **26** 331 (1971).;
[8] S. W. Hawking, *Phys. Rev. Lett.* **26** 1344 (1971).
[9] R. Wald, *Phys. Rev. Lett.* **26** 1653 (1971).
[10] B.Boisseau, P.Letelier, *Gen. Rel. Grav.* **34**,1077 (2002).
[11] J. Winicour, A.I. Janis and E.T. Newman *Phys. Rev.* **176**,1507 (1968).
[12] A. Janis, E.T Newman and J. Winicour *Phys. Rev. Lett.* **20**, 878 (1968).
[13] L. Bel *Gen. Relativ. Gravitation* **1**, 337 (1971).
[14] F. I. Cooperstock and G. J. Junevicius *Nuovo Cimento* **16B**, 387 (1973).
[15] L. Herrera *Int. J. Mod. Phys. D* **17** , 557 (2008).
[16] L. Herrera *Int. J. Mod. Phys. D* **17** , 2507 (2008).
[17] R. Bach and H. Weyl, *Math. Z.*, **13**, 134 (1920).
[18] G. Darmais, *Les equations de la Gravitation Einsteinienne* (Gauthier-Villars, Paris) P.36, (1927).
[19] D.M. Zipoy, *J. Math. Phys.*, **7**, 1137 (1966).
[20] R. Gautreau and J. L. Anderson, *Phys. Lett.*, **25A**, 291 (1967).
[21] F.I. Cooperstock and G.J. Junevicius, *Int. J. Theor. Phys.*, **9**, 59 (1968).
[22] B.H. Vorhees, *Phys. Rev. D*, **2**, 2119 (1970).
[23] F. Espósito and L. Witten, *Phys. Lett.*, **58B**, 357 (1975).
[24] K.S. Virbhadra, *gr-qc/9606004*.
[25] J. L. Hernández-Pastora and J. Martín, *Gen. Rel. Grav.* **26**, 877 (1994).
[26] J. L. Hernández-Pastora, J. Martín and E. Ruiz *Gen. Rel. and Grav.* **30**, 999 (1998).
[27] L. Herrera, F. Paiva and N. O. Santos, *Int. J. Modern Phys.D* **9**, 649 (2000).
[28] L. Herrera, *Foun. Phys. Lett.* **18**, 21 (2005).
[29] L. Herrera, A. Di Prisco and J. Martinez, *Astr. Space Sci.* **277**, 447 (2001).
[30] L. Herrera, A. Di Prisco and E. Fuenmayor, *Class. Quantum Grav.* **20**, 1125 (2003).
[31] K. S. Virbhadra, D. Narashima and S. M. Chitre, *Astron. Astrophys.* **337**, 1 (1998).
[32] K. S. Virbhadra, and G. F. R. Ellis, *Phys. Rev. D* **65**, 103004 (2002).
[33] K. S. Virbhadra and C. R. Keeton, *Phys. Rev. D* **77**, 124014 (2008).
[34] G. N. Gyulchev and S. S. Yazadjiev, *Phys. Rev. D* **78**, 083004 (2008).
[35] C. Bambi and K. Freese, *Phys. Rev. D* **79**, 043002 (2009).

- [36] K. Hioki and K. I. Maeda, *Phys. Rev. D* **80**, 024042 (2009).
- [37] C. Bambi, K. Freese, T. Harada, R. Takahashi and N. Yoshida *Phys. Rev. D* **80**, 104023 (2009).
- [38] C. Bambi, T. Harada, R. Takahashi and N. Yoshida *Phys. Rev. D* **81**, 104004 (2010).
- [39] Z. Stuchlik and J. Schee, *Classical Quantum Gravity* **27**, 215017 (2010).
- [40] Z. Kovacs and T. Harko, *Phys. Rev. D* **82**, 124047 (2010).
- [41] D. Pugliese, H. Quevedo and R. Ruffini *Phys. Rev. D* **84**, 044030 (2011).
- [42] P. Pradhan and P. Majumdar *Phys. Lett. A* **375**, 474 (2011).
- [43] A. N. Chowdhury, M. Patil, D. Malafarina and P. S. Joshi *Phys. Rev. D* **85**, 104031 (2012).
- [44] C. Bambi and G. Lukes-Gerakopoulos, *Phys. Rev. D* **87**, 083006 (2013).
- [45] J.H. Young and C. A. Coulter, *Phys. Rev.* **184**, 1313 (1969).
- [46] D. Bini, C. Cherubini, S. Filippi and A. Geralico, *Gen. Rel. Grav.* **41**, 2781, (2009).
- [47] H. Quevedo and B. Mashhoon, *Phys. Lett. A* **109**, 13 (1985).
- [48] D. Bini, A. Geralico, O. Luongo and H. Quevedo, *Classical Quantum Gravity*, **26**, 225006, (2009).
- [49] V. S. Manko and I. D. Novikov, *Classical Quantum Gravity* **9**, 2477 (1992).
- [50] J. L. Hernández-Pastora *Classical Quantum Grav.* **30**, 175003 (2013).
- [51] R. Geroch, *J. Math. Phys.* **11**, 1955 (1970)
- [52] R. Geroch, *J. Math. Phys.* **11**, 2580 (1970)
- [53] K. S. Thorne, *Rev. Mod. Phys.* **52**, 299 (1980)
- [54] G. Fodor, C. Hoenselaers and Z. Perjés, *J. Math. Phys.*, **30**, 2252, (1989).
- [55] M. Herberthson, *Classical Quantum Gravity* **21**, 5121 (2004).
- [56] T. Bäckdahl and M. Herberthson, *Classical Quantum Gravity* **22**, 3585 (2005).
- [57] T. Bäckdahl and M. Herberthson, *Classical Quantum Gravity* **23**, 5997 (2006).
- [58] Hernández-Pastora, J.L., *Ph.D. Relativistic gravitational fields close to Schwarzschild solution*, Universidad de Salamanca. (1996).
- [59] T. Bäckdahl and M. Herberthson, *Classical Quantum Gravity* **22**, 1607 (2005).
- [60] L. Herrera and J. L. Hernández-Pastora, *J. Math. Phys.* **41**, 7544 (2000)
- [61] J. L. Hernández-Pastora and J. Ospino, *Phys. Rev. D* **82**, 104001 (2010).
- [62] L. Herrera, J. Carot, N. Bolivar and E. Lazo, *Int.J.Theor.Phys.* **48**, 3537 (2009)
- [63] L. Herrera, W. Barreto and J. L. Hernández-Pastora, *Gen. Relativ. Gravit.* **37**, 873 (2005)
- [64] H. Quevedo *Fortschr. Phys.* **38**, 733 (1990).
- [65] A. F. Teixeira *Progr. Theor. Phys.* **60**, 163 (1978).
- [66] S. Kato, J. Fukue and S. Mineshige *Black-hole Accretion Disks* (Kyoto University Press, Kyoto), (1998).